



ALMA MATER STUDIORUM
UNIVERSITÀ DI BOLOGNA

Attenuation Tomography Analysis in the Val d'Agri Oilfield

Martina Avella¹, Luca De Siena¹, Alexander Garcia², Lucia Zaccarelli²

¹Alma Mater Studiorum - Università di Bologna, Dipartimento di Fisica e Astronomia "Augusto Righi", Bologna, Italy;

²Istituto Nazionale di Geofisica e Vulcanologia, Department of Bologna, Bologna, Italy



1. Aim

The Val d'Agri basin is a unique natural laboratory where industrial fluid operations intersect with natural seismicity. By imaging attenuation, a proxy for fluid content and rock damage, this work aims to advance our ability to monitor subsurface changes, improving both resource management and seismic risk assessment in active hydrocarbon systems worldwide.

2. Study Area and Geology

Tectonic Setting

Quaternary extensional basin in the southern Apennines, superimposed on a compressional fold-and-thrust belt. Europe's largest onshore hydrocarbon system and a well-documented site of induced seismicity.

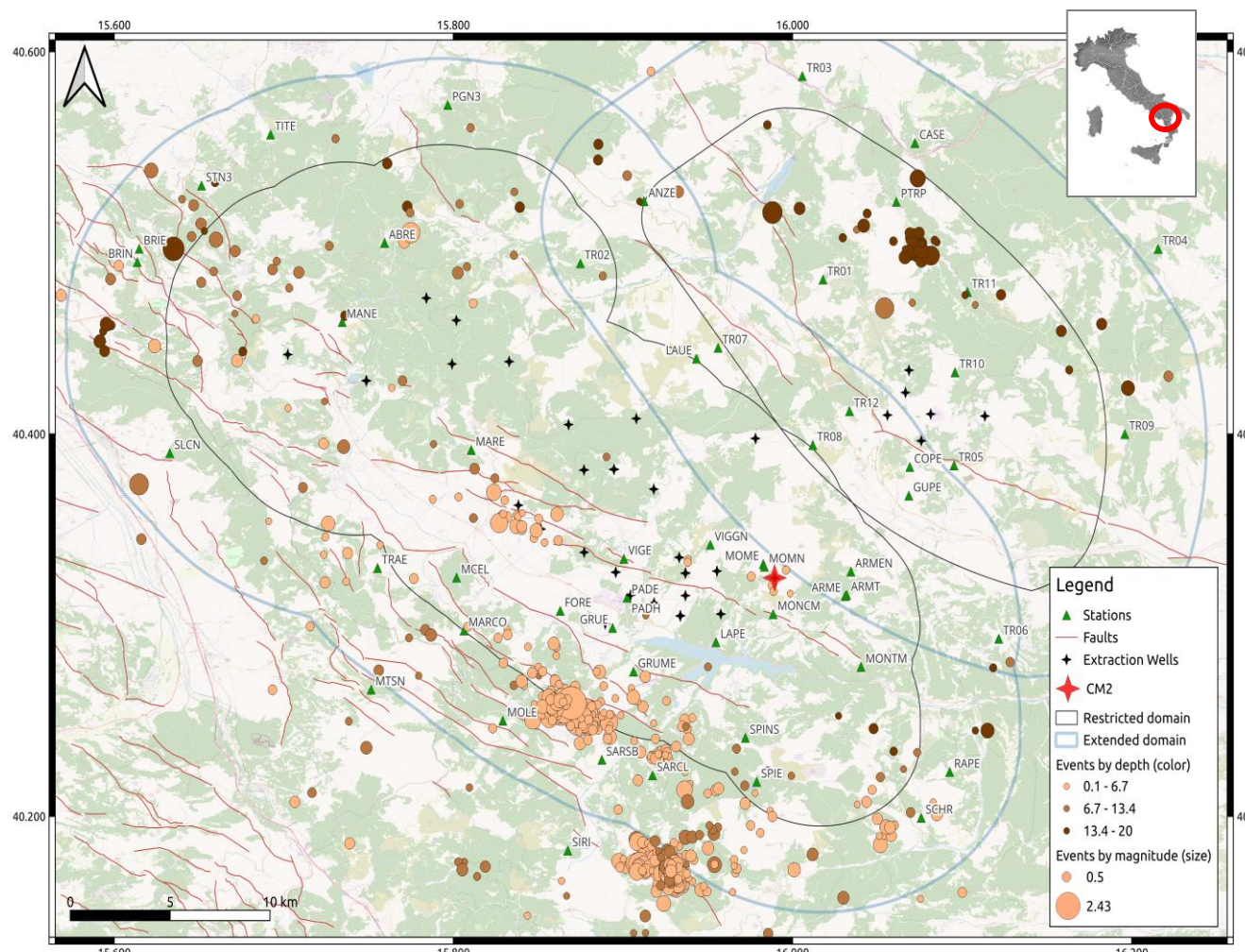
Stratigraphy & Reservoirs

Reservoir hosted in Mesozoic carbonates (Lagonegro Basin & Apulia Platform) at 2–7 km depth, overlain by Miocene–Pliocene flysch and Quaternary clastics. Two structurally isolated compartments:

- **Val d'Agri (VA)**: 2–4 km depth, shallow carbonate culmination (larger western domain)
- **Tempa Rossa (TR)**: 5–7 km depth, deeper isolated block (smaller eastern domain)

Industrial Activity & Seismicity

- **Costa Molina 2 (CM2) Injection Well**: Wastewater injection at 2,890–3,096 m into the VA fault damage zone
- **Seismicity**: 664 events, 8,433 station-event pairs, $0.5 < M < 2.5$
- **Production Network**: Extraction wells in both fields; long-term depletion modifies crustal stress and fracture networks



Local seismicity (2020–2025) overlaid on topography, active faults, and monitoring domains.

Dataset

Local earthquake catalog (2020–2025), dense station coverage, optimal ray paths through the 2–6 km reservoir interval.

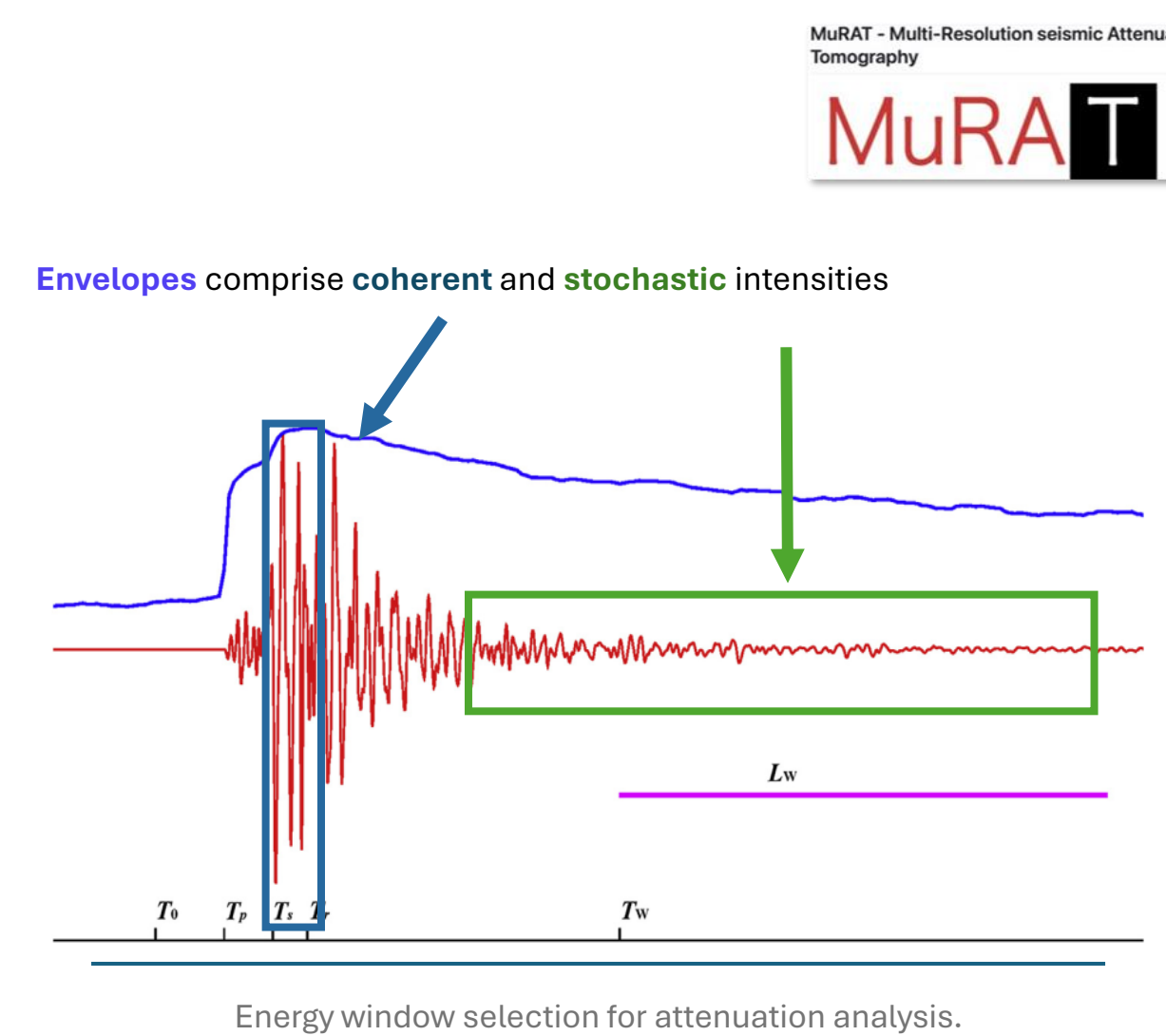
3. Method

MuRAT4 Framework

Multi-Resolution seismic Attenuation Tomography (MuRAT4) provides a multi-parameter description of seismic energy loss.

What We Measure:

- **Peak Delay (PD)**: Time shift of peak amplitude relative to reference; mainly sensitive to **scattering** by heterogeneities
- **Q (Total Attenuation)**: Amplitude decay of direct waves; captures combined **scattering + absorption**
- **Qc (Coda Attenuation)**: Decay rate of coda wave envelope; primarily reflects **intrinsic absorption** (fluid/thermal losses)
- **Multi-Frequency Analysis**: Simultaneous inversion at 6, 12, and 18 Hz to constrain scale-dependent structures



Key Improvements in MuRAT 4.0:

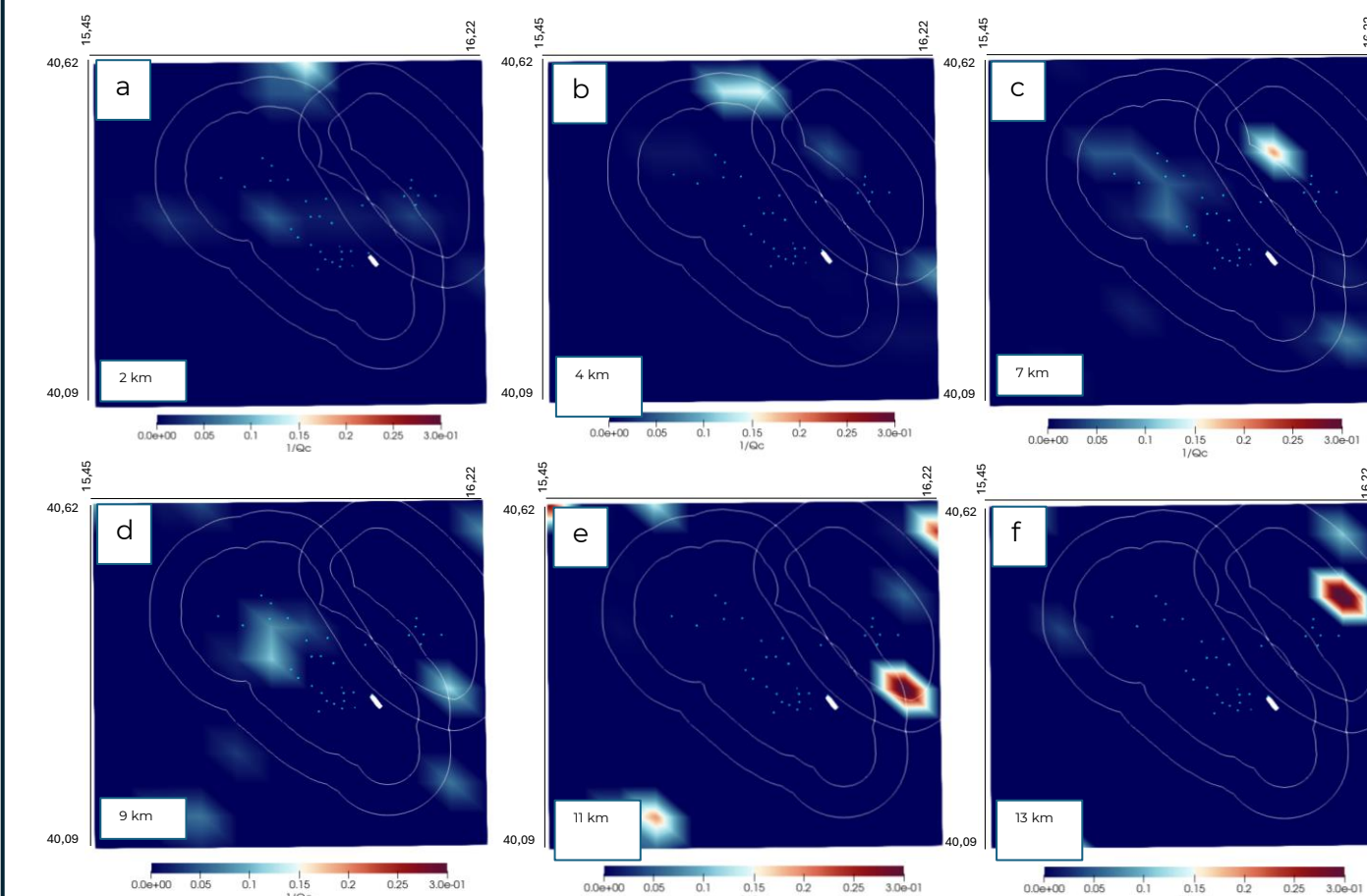
- **Differential kernels**: Numerically calculated sensitivity for stable contrast resolution (~2 orders of magnitude)
- **Frequency-dependent damping**: Explicit smoothing/damping parameters per frequency band
- **Positivity constraint**: Guarantees physical, non-negative Q and Qc values
- **Enhanced validation**: Stricter enforcement of diffusive regime, energy conservation, and coda-stability assumptions

Resources:

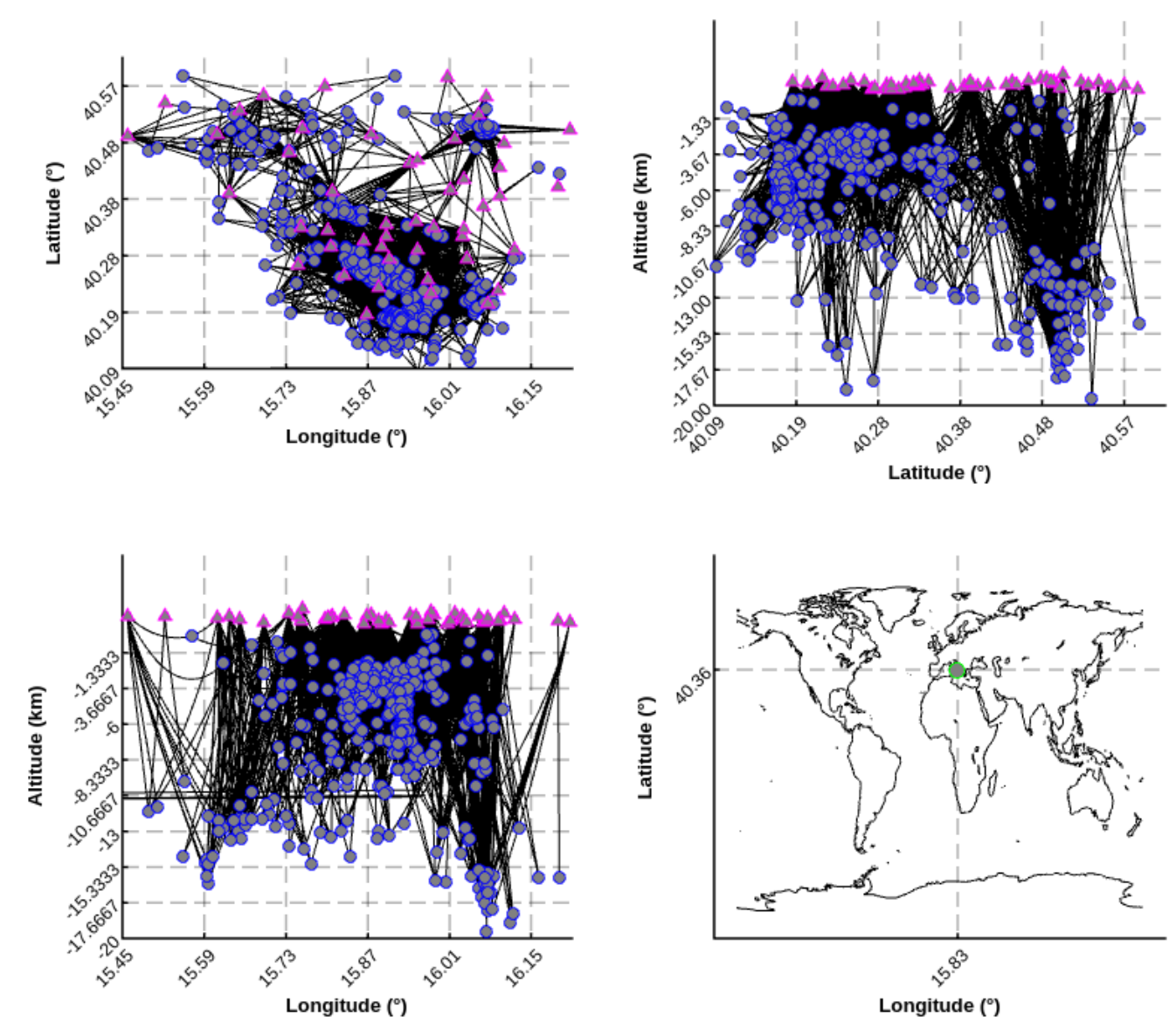
MuRAT4 is available at github.com/LucaDeSiena/MuRAT

4. Results

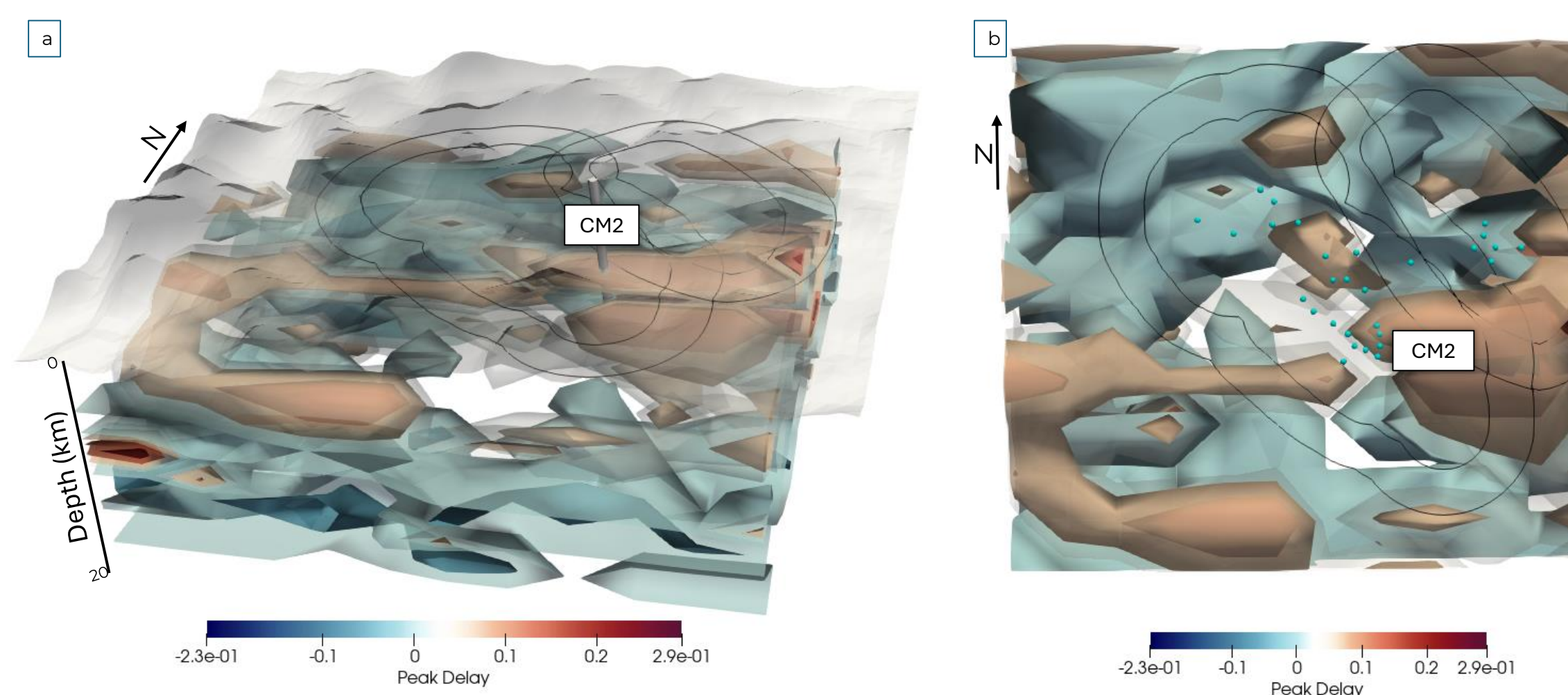
MuRAT4.0



3D coda attenuation (Qc) distribution at 12 Hz across six depth slices. Red: high attenuation (low Qc). Blue: low attenuation (high Qc). Light blue points: extraction wells. White cylinder: extraction well CM2.



Ray-path density and hypocentre distribution used in tomographic inversion. Dense crossing geometry ensures robust sampling of the reservoir volume. Declustered dataset optimised for coda stability and uniform spatial coverage.



3D volume rendering of the 12 Hz Peak Delay model. The injection well CM2 is indicated in both images as a white cylinder. b) The light blue dots represent the extraction wells

MuRAT4.0 Processing Parameters (Val d'Agri)

Peak Delay (Scattering):

- Window: 0.1–4 s; selection threshold = 2 σ from average trend
- Regionalisation weighted by ray length (no forward inversion)

Coda Attenuation (Qc):

- Lapse time method: Constant (start = 10 s, window = 10 s)
- Measurement: Non-linear grid search (fit threshold $R^2 \geq 0.006$)
- Inversion parameters (frequency-dependent):
 - Albedo (B_0): [0.1, 0.2, 0.1] @ [6, 12, 18] Hz
 - Inverse extinction length: [0.1, 0.09, 0.08] km⁻¹
- Kernel threshold = 2 (computational grid refinement)

Solver: **Tikhonov** inversion via MATLAB Optimization Toolbox

- Positivity constraint enforced (non-negative Q, Qc)

Frequency-dependent damping:

- Qc: [0.3, 0.3, 0.1]
- Q: [0.001, 0.001, 0.001]
- Smoothing: [0, 0, 0] (no additional spatial smoothing)

Inversion grid:

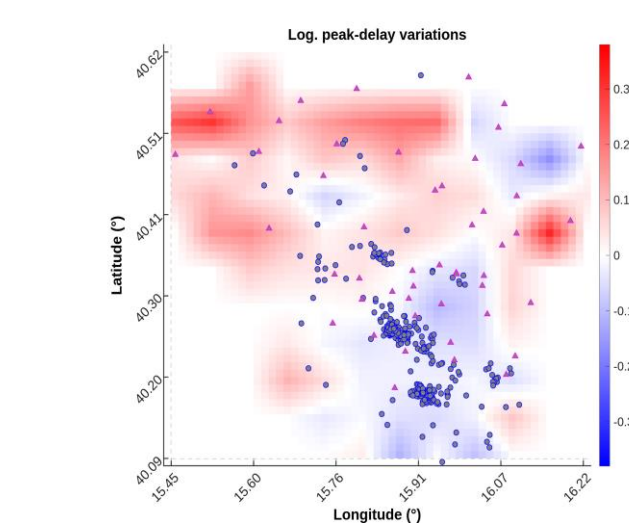
- 12 × 12 × 10 nodes (Lat × Lon × Depth)
- Extent: 40.09–40.62°N, 15.45–16.22°E, +1 to –20 km depth

Validation:

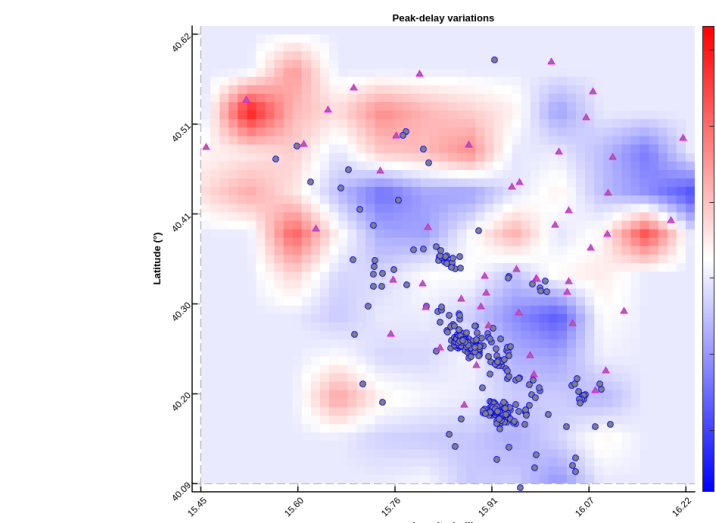
- Checkerboard test: anomaly size = 2 × node spacing
- Spike test: location [40.30–40.40°N, 15.80–16.10°E, –6 to –16 km]
- Picard condition analysis for parameter resolution

5. Comparison

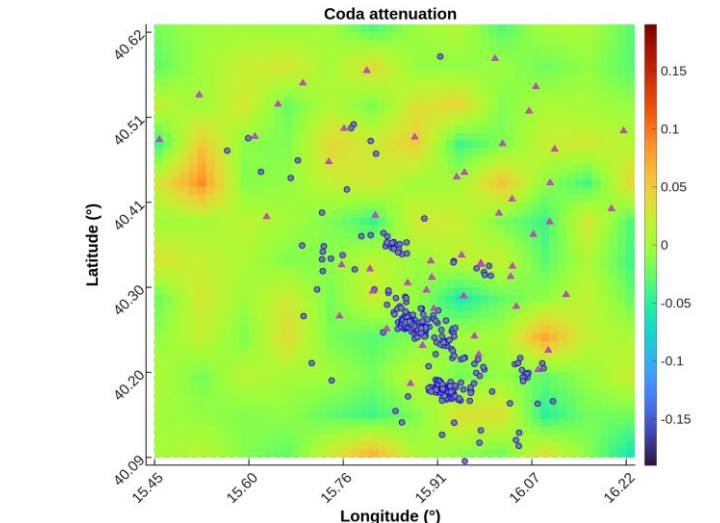
| Feature | MuRAT 3.0 | MuRAT 4.0 |
|---------------------------------|---|--|
| Inversion Solver | IRTools / Tikhonov, Hybrid | regtools MATLAB Optimization Toolbox (this study uses Tikhonov with positivity constraint) |
| Inversion Parameters | Fixed scalar values (e.g., albedo = 0.5, Le = 0.02 km ⁻¹) | Frequency-dependent arrays (albedo & inverse extinction length defined per frequency band) |
| Sensitivity Kernels | Absolute diffusive kernels (Del Pezzo et al., 2018) | Differential kernels (Del Pezzo-based); updated philosophy yields realistic contrast resolution (~2 orders of magnitude) vs. unstable 6–7 orders in v3 |
| Peak Delay Imaging | Regionalization via hit-count weighting | Same regionalization approach, now explicitly weighted by ray length (no forward inversion; preserves structural sensitivity) |
| Validation & Physics | Standard Picard condition & L-curve damping | Enhanced physical-consistency checks; stricter enforcement of diffusive regime, energy conservation, and coda-stability assumptions |



MuRAT 3.0 peak-delay variations regionalised via simple hit-count weighting. Serves as reference for structural sensitivity before ray-length weighting implementation.



MuRAT 4.0 peak delay variations regionalised with explicit ray-length weighting.



MuRAT 3.0 coda attenuation map at 7 km depth for direct comparison. Uses absolute diffusive kernels and fixed MLTWA parameters. Highlights baseline resolution prior to MuRAT 4.0 improvements.

6. Conclusions

- MuRAT 4.0 introduces **critical methodological upgrades** over v3.0, including **differential sensitivity kernels, positivity-constrained inversion, and frequency-dependent inversion parameters**.
- These improvements enforce stricter **physical consistency**, ensuring better adherence to diffusive regime assumptions, energy conservation, and coda-stability criteria.
- Enhanced numerical stability and realistic contrast resolution (~2 orders of magnitude) yield **more reliable tomographic images** for complex reservoir systems.
- With its robust optimisation framework and improved validation protocols, MuRAT 4.0 is positioned to replace v3.0 as the **new standard for multi-resolution attenuation tomography**.

7. References

De Siena L., Calvet, M., Watson, K.J., Jonkers, A.R.T. and Thomas, C., 2016. Seismic scattering and absorption mapping of debris flows, feeding paths, and tectonic units at Mount St. Helens volcano. *Earth and Planetary Science Letters*, 442, pp.21–31

De Siena L., A. Amoroso, E. Del Pezzo, Z. Wakeford, M. Castellano, L. Crescentini, 2017. Space-weighted seismic attenuation mapping of the aseismic source of Campi Flegrei 1983–94 unrest. *Geophysical Research Letters*, 44, 4, pp. 1740–1748.

Del Pezzo, E., De La Torre, A., Bianco, F., Bianco, Z., Cabrelli, S., and De Siena, L. (2018). Numerically Calculated 3D Space-Weighting Functions to Image Crustal Volcanic Structures Using Diffuse Coda Waves. *Journal of Geophysical Research: Solid Earth*, 123, 9050–9062. <https://doi.org/10.1029/2017JB014722>

Napolitano, F., De Siena, L., Amoroso, O., Agüstsóttir, T., Benediktsdóttir, A., Palo, M., et al. (2025). Scattering and absorption imaging of the Hengill high-temperature geothermal area, southwest Iceland. *Journal of Geophysical Research: Solid Earth*, 130, e2024JB030731. <https://doi.org/10.1029/2024JB030731>

Lavecchia, G., Bello, S., Cirillo, D., Pietrolungo, F., & Brozzetti, F. (2023). Quaternary-Holocene Fault Database 2.0 (Southern Italy) [Data set]. Zenodo. <https://doi.org/10.5281/zenodo.10370819>

Improta, L., Bagh, S., De Cori, P., Valeroso, L., Pastori, M., Piccinini, D., ... Buttinelli, M. (2017). Reservoir structure and wastewater-induced seismicity at the Val d'Agri oilfield (Italy) shown by three-dimensional Vp and Vp/Vs local earthquake tomography. *Journal of Geophysical Research: Solid Earth*, 122, 9050–9062. <https://doi.org/10.1029/2017JB014722>

Luca De Siena, mressissi, Y. Zhang, Donato Taloni, Azeel Abbas, WMZ, Cheng Qingyang, Ferdinando Napolitano, & Simona Gabrielli. (2026). LucaDeSiena/MuRAT: Legacy MuRAT3.0 Code (v3.26.01.20). Zenodo. <https://doi.org/10.5281/zenodo.18316669>

De Siena, L. (2026). MuRAT4: Multi-Resolution seismic Attenuation Tomography (Version 4.0) [Software]. GitHub. <https://github.com/LucaDeSiena/MuRAT/tree/MuRAT4>

